Interacting Slow and Fast Dynamics in Precise Spiking-Bursting Neurons

Fabiano Baroni[1], Joaquin J. Torres[2], and Pablo Varona[1]

[1] Grupo de Neurocomputación Biológica (GNB),
Dpto. de Ingeniería Informática,
Escuela Politécnica Superior,
Universidad Autónoma de Madrid,
28049 Madrid, Spain
{fabiano.baroni, pablo.varona}@uam.es
[2] Departamento de Electromagnetismo y Física de la Materia,
Universidad de Granada, 18071 Granada, Spain
Institute Carlos I for Theoretical and Computational Physics,
Universidad de Granada 18071 Granada, Spain
jtorres@onsager.ugr.es

Abstract. We have explored the role of the interaction of slow and fast intracellular dynamics in generating precise spiking-bursting activity in a model of the heartbeat central pattern generator of the leech. In particular we study the effect of calcium-dependent currents on the neural signatures generated in the circuit. These neural signatures are cell-specific interspike intervals in the spiking-bursting activity of each neuron. Our results show that the slow dynamics of intracelullar calcium concentration can regulate the precision and shape of the neural signatures.

1 Introduction

There are many different intracellular dynamics that directly or indirectly influence the electrical activity of neurons [1, 2, 3]. These different dynamics can act in several timescales. The combination of ionic currents with different kinetics and time constants are responsible, for example, of the characteristic spiking-bursting activity of many central pattern generator neurons. Some of these channels are fast and affect the action potential generating mechanisms of the cells. Other channels are slow and regulate the burst depolarization waves. Calcium dynamics is often considered to affect mainly the slow depolarization waves. However, the interaction of fast and slow dynamics gives rise to phenomena on both time scales.

A Central Pattern Generator (CPG) is a neural network that, acting alone or together with other CPGs, drives a motor movement that must be repeated in time. CPG neurons are typically spiking-bursting cells [4, 5, 6, 7] that generate a characteristic rhythmical pattern of activity. The signal produced by a CPG consists of a sequence of rhythmic bursts of action potentials. Typically, it is

thought that the intraburst spike structure is not important to characterize the CPG behavior and its communication with other external neurons and systems. However, recent studies using in vitro preparations [8] have revealed that each neuron of the pyloric CPG of the lobster has a specific individual neural signature that coexists with its characteristic slow rhythm. These signatures consist of a cell-specific interspike interval (ISI) distribution. The origin of these signatures has been studied using model networks [9, 10, 11]. In these models the synaptic configuration of the network is the main factor shaping the signatures, although the intrinsic dynamics of each cell can also contribute to the specific ISI distributions.

In this paper we assess the influence of slow calcium dynamics on the generation and precision of neuronal signatures. We study this using a model of a well-known CPG: the circuit pacing the heartbeat of the medicinal leech, *Hirudo medicinalis*. The main neurons of this circuit are modeled with a previously developed Hodgkin-Huxley type formalism in which we include dependence upon calcium concentration in an outward potassium current.

2   CPG Model

The rhythmic activity of the leech heartbeat CPG originates from two segmental oscillators located in the third and fourth midbody ganglia, each one formed by a couple of reciprocally inhibiting heart interneurons, called oscillator interneurons [12]. The interneurons located in the first and second ganglion act to coordinate the activity of the two segmental oscillators, and are then referred to as coordinating interneurons [13, 14, 15]. The system exhibits a symmetry between the third and the fourth ganglion, so that only a couple of heart oscillator interneurons are depicted in the schematic representation of the circuit shown in Fig. 1A. Leech heart interneurons are commonly referred to with a nomenclature indicating the emibody and the ganglion where they are located, and we will use this nomenclature throughout the paper.

We depart from a conductance-based model developed by the Calabrese group [16]. The general equation that describes the membrane potential of each model neuron is the following:

$$C_m \frac{dV}{dt} = -(I_l + I_{SynS} + I_{SynG} + I_{ion}) \tag{1}$$

where C_m is the total membrane capacitance, I_l is a leakage current, I_{SynS} is the spike-mediated synaptic current, I_{SynG} is the graded synaptic current, and

$$I_{ion} = I_{Na} + I_P + I_{CaF} + I_{CaS} + I_h + I_{K1} + I_{K2} + I_{KA} \tag{2}$$

is the total ionic current for oscillator heart interneurons. For the coordinating heart interneurons:

$$I_{ion} = I_{Na} + I_{K1} + I_{K2} \tag{3}$$

Five inward currents are included in the oscillator interneuron model: a fast Na^+ current I_{Na}, a persistent Na^+ current I_P, a fast, low-threshold Ca^{2+} current I_{CaF}, a slow, low-threshold Ca^{2+} current I_{CaS}, and a hyperpolarization-activated cation current I_h [17, 18, 19, 20]. Three outward currents are also included: a delayed rectifier like K^+ current I_{K1}, a persistent K^+ current I_{K2}, and a fast K^+ transient current I_{KA}. Each of these currents have Hodgkin-Huxley type kinetics. Coordinating model interneurons implement only a subset of the ionic currents described for oscillator heart interneurons. For a complete description of the model see [16].
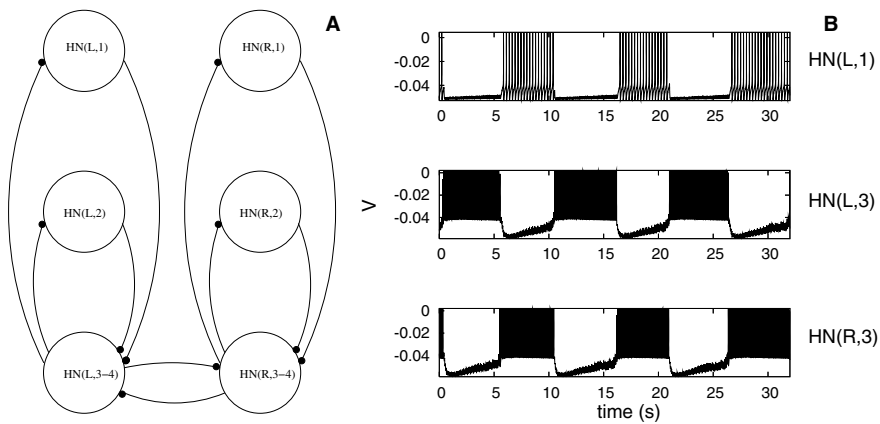
Fig. 1. A schematic representation of the circuit and electrical activity of the CPG model. A: the timing network contains four pairs of bilaterally symmetric interneurons that have cell bodies in the first four midbody ganglia (G1 to G4). The representations of oscillator heart interneurons in the 3rd and 4th ganglia are combined. Open circles represent cell bodies and lines ending in small filled circles represent inhibitory synapses. B: from top to bottom: voltage traces of heart interneurons HN(L,1), HN(L,3), HN(R,3)

This model produces rhythmic oscillations (Fig. 1B) with a mean period of $10.4 \pm 0.2s$. Several studies have pointed out the role of presynaptic calcium concentration in graded [21] and spike-mediated [22] synaptic transmission among oscillator interneurons coupled in a half center oscillator, while no existing model takes into account homeostatic regulation of ionic conductances based upon calcium concentration in this circuit. Nevertheless, calcium dependent potassium conductances have been described in several other cells in the leech nervous system, such as Retzius [23], anterior pagoda [24], and anterior lateral giant [25], and might be ubiquitous in invertebrate neurons. The modifications that we perform on the original model [16] (described below) are meant to incorporate calcium dependence in the activation variable of the persistent (non-inactivating) potassium current I_{K2}. We chose this among the three potassium currents described in the original model because its relatively slow kinetics makes it vary on a time

scale closer to the burst time scale than to the individual spike time scale, albeit incorporation of the same kind of calcium dependent regulation on the kinetics of I_{K1} activation variable leads to similar results (data not shown). Nevertheless this study is meant to be more a prove of principle of what might be the influence of slow homeostatic regulation of ionic conductances on burst temporal structure than a biophysically realistic description of the subcellular mechanism underlying this regulation. We implemented calcium dependence upon the activation variable of I_{K2} as a calcium dependent voltage shift V_{shift} in the steady state and time constant of the activation function:

$$m_{\infty,K2} = \frac{1}{1 + \exp(-83(V + V_{shift} + 0.02))} \tag{4}$$

$$\tau_{m,K2} = 0.057 + \frac{0.043}{1 + \exp(200(V + V_{shift} + 0.035))} \tag{5}$$

where V_{shift} is calculated according to the equation:

$$V_{shift} = k \cdot \ln(\frac{[Ca^{2+}]_{eff}}{[Ca^{2+}]_{eff_0}}) \tag{6}$$

We chose $k = 0.002V$ and $[Ca]_{eff_0} = 1.36 \cdot 10^{-12}$. An additional equation describes the dynamics of intracellular effective calcium concentration,

$$\frac{d[Ca^{2+}]_{eff}}{dt} = \frac{I_{Ca} - B[Ca^{2+}]_{eff}}{\tau_C} \tag{7}$$

where

$$I_{Ca} = \max(0, -I_{CaF} - I_{CaS}) \tag{8}$$

In Eq. 7 parameter B is a buffering rate constant and τ_C is a lumped time constant describing both calcium diffusion and the kinetics of binding/unbinding of calcium to receptors modulating the gating of I_{K2} ionic channels. It is important to note that $[Ca^{2+}]_{eff}$ is not necessarily meant to reproduce the actual calcium concentration in a concrete intracellular region, even if intracellular calcium concentration in the proximity of the cell membrane is surely rate limiting for $[Ca^{2+}]_{eff}$. This model will from now on be referred to as the calcium model, as opposed to the original model described in [16]. Note that the implementation of the coordinating interneurons and of the synaptic coupling is the same in the two models. The calcium model also produces a robust oscillatory rhythm (Fig. 2A) with a period of $6.16 \pm 0.07s$.

The models were implemented in C and equations were integrated with a variable step Runge-Kutta 6(5) integration routine for at least 950 burst in each cell. The first 100 seconds of simulated data were not included in the analysis. Spike times were collected and the corresponding ISIs were calculated as difference of successive spike times. ISI distributions in all cases were clearly bimodal, so it was possible to unambiguously define a burst threshold. Cycle period was calculated considering the semi-sum of the first and last spike time of each burst.

Two different forms of visualizing and quantifying burst structures were used: ISI return maps and ISI versus ISI index plots. ISI return maps were constructed by plotting each ISI against the previous ISI. For neurons with a robust bursting behavior as the one considered in this study, is it possible to uniquely determine an intraburst region in the ISI return map (corresponding to triplets of spikes belonging to the same burst) and two interburst regions (corresponding to triplets belonging to different bursts). ISI versus ISI index plots represent the mean and standard deviation of the ISI with the same index inside a burst, plotted against the ISI index. Indexes with less than three ISIs were not included in the analysis. Due to the symmetry of the model only results from one neuron of each kind are presented.

3   Results

Figure 2B shows the membrane potential of an oscillator interneuron together with the time course of $[Ca^{2+}]_{eff}$ and V_{shift}. As the cell depolarizes, Ca^{2+} enters through voltage dependent calcium channels and $[Ca^{2+}]_{eff}$ correspondingly rises until approximately one third of the whole duration of the burst. As $[Ca^{2+}]_{eff}$ rises, V_{shift} produces a shift towards a more hyperpolarized potential of the steady state and time constant curves of the I_{K2} activation function, resulting in a greater activation of this current. This corresponds to a $[Ca^{2+}]_{eff}$ dependent increase in the total repolarizing current, enhancing firing frequency adaptation along a burst (as we will discuss in Fig. 4C) and eventually causing a precocious escape from inhibition of the contralateral neuron and an overall increase in cycle frequency. This is consistent with the general intuition of calcium dynamics as a mechanism providing a delayed negative feedback to the dynamics of neuron models.

The calcium model generates bursts with a more precise temporal structure than the original model. Figure 3 shows the ISI return maps for an oscillator
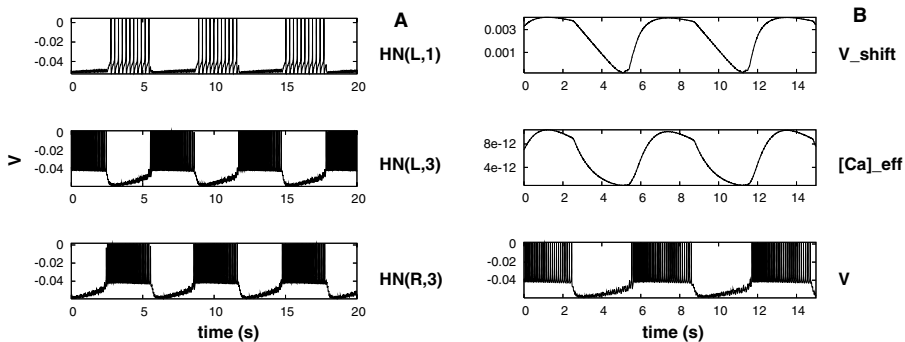
Fig. 2. Dynamics of the calcium model. Panel A, from top to bottom: voltage traces of heart interneurons HN(L,1), HN(L,3), HN(R,3). Panel B, from top to bottom: $[Ca^{2+}]_{eff}$, V_{shift} and voltage time course for oscillator interneuron HN(L,3)

and a coordinating interneuron in the two models. It is remarkable how the sparse triplets present in the intraburst region of the ISI return map of the coordinating interneuron HN(L,1) in the original model disappear in the calcium model, for which all intraburst triplets fall in a small interval. More detailed analysis revealed that those sparse triplets in the original model all share the feature of being the last triplets of a burst. The interburst regions for the two kinds of heart interneurons under study are both fairly more precise in the calcium model than in the original model (only interburst regions for oscillator interneurons are shown). This is consistent with the lower standard deviation in the cycle period for the calcium model.
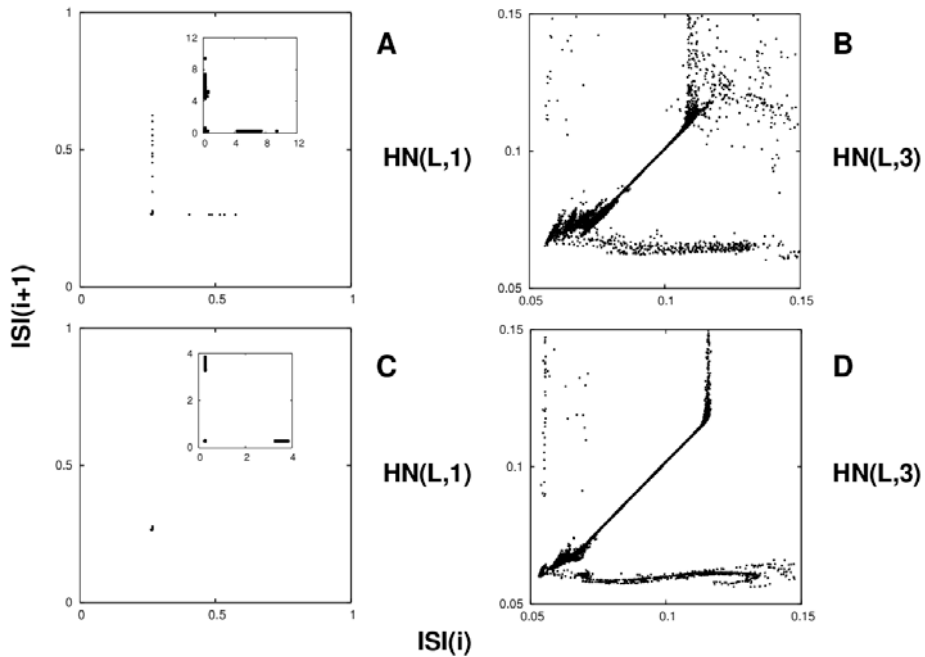
Fig. 3. Intraburst region of ISI return maps for the coordinating interneuron HN(L,1) (left) and the oscillator interneuron HN(L,3) (right) in the original (top) and calcium (bottom) models. Insets in A,C show full ISI return maps for coordinating interneuron HN(L,1) in the two models

The ISI return maps are useful to identify the correlation between successive ISIs. However, they do not provide detailed information about the distribution of each ISI index inside the burst. Thus, we also plot the mean and standard deviation of the ISIs against the ISI index inside a burst (Fig. 4A,C).

Besides the shorter cycle period in the calcium model, reflected in a smaller number of spikes per burst, two main features qualitatively differentiate the burst structure in the two models: the precision of the burst structure and the
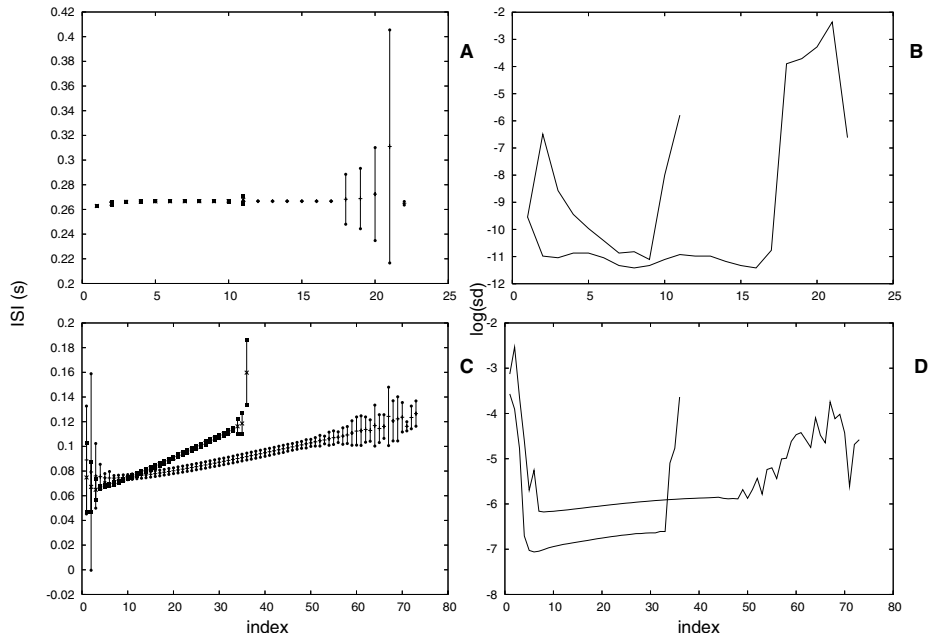
Fig. 4. Left panels: mean and standard deviation of ISI of the same index plotted against the index of the ISI inside a burst for HN(L,1) (top) and HN(L,3) (bottom) for the two models. Original model: mean ISI plotted with bars, errorbars ending with filled circles. Calcium model: mean ISI plotted with crosses, errorbars ending with filled squares. Right panels: standard deviation of ISI of the same index plotted in logarithmic scale against the index of ISI inside a burst for HN(L,1) (top) and HN(L,3) (bottom) for the two models. Original model: thin line. Calcium model: thick line

profile of the mean ISI along a burst. The coordinating interneurons do not differ in the two models, so that any change in the dynamics of these neurons in the two models is attributable only to network activity and not to intrinsic neuronal properties. Nevertheless, while the mean ISI for each index inside a burst is almost unchanged in the two models, ISI precision is slightly corrupted in the calcium model over all indexes except for the last indexes of the burst, for which the calcium model achieves enhanced precision (Fig. 4B). This is consistent with the previous observation that all intraburst triplets in the ISI return map for HN(L,1) in the calcium model are included in a small interval. Oscillator interneurons are the neurons where calcium dynamics was effectively added, so that any change in the dynamics of these neurons in the two models is attributable to both network activity and intrinsic neuronal properties. ISI precision for these neurons in the calcium model is greatly enhanced with respect to the original model for all possible ISI indexes inside a burst, except for the last ISI ending a burst. This improvement in ISI precision is particularly evident in Fig. 4D, where standard deviation of ISI with a given index is plotted against ISI

index inside a burst in logarithmic scale. Note that there is almost one order of magnitude of improved precision with respect to the original model. The mean of ISI with a given index increases along a burst with a higher slope in the calcium model than in the original model, reflecting the added spike time adaptation mechanism provided by the dependence of non-inactivating potassium channels upon calcium concentration.

4   Discussion

Bursts are traditionally considered as unitary events. The intraburst spike distribution of CPG neurons has not been analyzed in great detail since, typically, it is thought that the slow wave dynamics is the main factor shaping the rhythmic behavior of the system. However, several recent experimental and modeling results indicate that the temporal structure of the bursts can be important for CPG neurons [8, 9, 10, 11]. In particular, CPG cells could use the specific temporal structure of their fast dynamics, in addition to the phase and frequency of the slow wave, as an information encoding mechanism. In this study we have demonstrated how the modulation of an outward current by intracellular calcium can provide a model CPG with enhanced precision in its burst structure.

An interesting question about oscillator heart interneurons is whether they can present endogenous spiking-bursting activity when they are pharmacologically isolated. It has been reported that this behavior can be achieved in the original model neuron only in a narrow region of the parameter space (E_{leak}, g_{leak}), i.e. the reversal potential and maximal conductance of the leak current, respectively [28]. Endogenous bursting has remarkable consequences on the activity of the timing network, ensuring robust bursting characteristics such as period, phase, and duty cycles in face of weakening of mutual inhibition or random or imposed changes in membrane parameters [28]. In fact, robust pacing rhythm with little sensitivity to parameter change has been observed in the living system but not in the original model.

A key question in this context is whether the consideration of an intracellular calcium dynamics modulating the conductances of outward currents can induce spiking-bursting activity in the single neuron model for a broader range of parameters, thus ensuring robust dynamics in the model network. Preliminary results in our neuron model show that coupling of intracellular calcium dynamics with the activation of I_{K2} potassium current can induce robust spiking-bursting behavior similar to that reported in the experiments. Nevertheless it has been reported that the addition of a FMRFamide-activated potassium current [27] with Hodgkin-Huxley like kinetics also produces an expansion of the bursting region for the single neuron model. Thus, future analysis will aim at assessing if the enhanced robustness observed in the calcium model can be attributable only to a net increase in total outward currents during the burst phase of a neuron's activity or if the modulation of outward currents by calcium concentration along a burst plays a key role in ensuring correct bursting activity over a wide range of parameters.

Further work will assess how the improved precision of the spiking-bursting activity depends on parameter values and on the specific implementation of calcium dependence on potassium channel conductances, how it relates to single neuron's activity, and to which extent it is functionally relevant to the dynamics of the network. Comparison with experimental data will test the physiological plausibility of our modeling choices and guide future research.

References

1. Berridge M.J. 1998. Neuronal calcium signaling. Neuron, 21: 13–26.
2. Varona P., Torres J.J., Abarbanel H.D.I., Rabinovich M.I., Elson R.C. 2001a. Dynamics of two electrically coupled chaotic neurons: Experimental observations and model analysis. Biological Cybernetics, 84 (2): 91–101.
3. Varona P., Torres J.J., Huerta R., Abarbanel H.D.I., Rabinovich M.I. 2001b. Regularization mechanisms of spiking-bursting neurons. Neural Networks, 14: 865–875.
4. Hartline, D. K. and Maynard, D. M. 1976. Motor patterns in the stomatogastric ganglion of the lobster panulirus argus. J Exp Biol, 62(2): 405–420.
5. Russell, D. F. and Hartline, D. K. 1978. Bursting neural networks: a reexamination. Science, 200(4340): 453–456.
6. Marder E. and Calabrese R.L. 1996. Principles of rhythmic motor pattern generation. Physiol Rev, 76: 687–717.
7. Selverston, A. I., Elson, R. C., Rabinovich, M. I., Huerta, R., and Abarbanel, H. D. I. 1998. Basic principles for generating motor output in the stomatogastric ganglion. Ann. N.Y. Acad. Sci, 860(1): 35–50.
8. Szucs, A., Pinto, R. D., Rabinovich, M. I., Abarbanel, H. D. I., and Selverston, A. I. 2003. Synaptic modulation of the interspike interval signatures of bursting pyloric neurons. J Neurophysiol, 89: 1363–1377.
9. Latorre, R., Rodriguez, F. B., and Varona, P. 2002. Characterization of triphasic rhythms in central pattern generators (i): Interspike interval analysis. Lect. Notes Comput. Sc., 2415: 160–166.
10. Rodriguez, F. B., Latorre, R., and Varona, P. 2002. Characterization of triphasic rhythms in central pattern generators (ii): Burst information analysis. Lect. Notes Comput. Sc., 2415: 167–173.
11. Latorre, R., Rodriguez, F. B., and Varona, P. 2004. Effect of individual spiking activity on rhythm generation of central pattern generators. Neurocomputing, 58-60: 535–540.
12. Peterson EL. 1983a Generation and coordination of heartbeat timing oscillation in the medicinal leech. I. Oscillation in isolated ganglia. J. Neurophysiol. 49: 611–626.
13. Peterson EL. 1983b Generation and coordination of heartbeat timing oscillation in the medicinal leech. II. Intersegmental coordination. J. Neurophysiol. 49: 627–638.
14. Hill AA, Masino MA, Calabrese RL. 2002. Model of intersegmental coordination in the leech heartbeat neuronal network.J Neurophysiol. 87(3):1586–602.
15. Jezzini SH, Hill AAV, Kuzyk P, Calabrese RL. 2004. Detailed model of intersegmental coordination in the timing network of the leech heartbeat central pattern generator. J. Neurophysiol. 91: 958–977.

16. Hill A.A.V., Lu J., Masino M.A., Olsen O.H., Calabrese R.L. 2001. A model of a segmental oscillator in the leech heartbeat neuronal network. Journal of Computational Neuroscience 10: 281–302.

17. Angstadt JD, Calabrese RL. 1989. A hyperpolarization-activated inward current in heart interneurons of the medicinal leech. J. Neurosci. 9: 2846–2857.

18. Angstadt JD, Calabrese RL. 1991. Calcium currents and graded synaptic transmission between heart interneurons of the leech. J. Neurosci. 11: 746–759.

19. Olsen OH, Calabrese RL. 1996. Activation of intrinsic and synaptic currents in leech heart interneurons by realistic waveforms. J. Neurosci. 16: 4958–4970.

20. Opdyke CA, Calabrese RL. 1994. A persistent sodium current contributes to oscillatory activity in heart interneurons of the medicinal leech. J. Comp. Physiol. A 175: 781–789.

21. Ivanov AI, Calabrese RL. 2000. Intracellular Ca2+ dynamics during spontaneous and evoked activity of leech heart interneurons: low-threshold Ca currents and graded synaptic transmission. J Neurosci. 20(13): 4930–43.

22. Ivanov AI, Calabrese RL. 2003. Modulation of spike-mediated synaptic transmission by presynaptic background Ca2+ in leech heart interneurons. J Neurosci. 23(4): 1206–18.

23. Beck A, Lohr C, Nett W, Deitmer JW. 2001. Bursting activity in leech Retzius neurons induced by low external chloride. Pflugers Arch. 442(2): 263–72.

24. Wessel R, Kristan WB Jr, Kleinfeld D. 1999. Dendritic Ca(2+)-activated K(+) conductances regulate electrical signal propagation in an invertebrate neuron. J Neurosci. 19(19): 8319–26.

25. Johansen J, Yang J, Kleinhaus AL. 1987. Voltage-clamp analysis of the ionic conductances in a leech neuron with a purely calcium-dependent action potential. J Neurophysiol. 58(6): 1468–84.

26. Calabrese RL, Nadim F, and Olsen OH. 1995. Heartbeat control in the medicinal leech: a model system for understanding the origin, coordination, and modulation of rhythmic motor patterns. J Neurobiol 27: 390–402.

27. Nadim F, Calabrese RL. 1997. A slow outward current activated by FMRFamide in heart interneurons of the medicinal leech. J. Neurosci. 17:4461–4472.

28. Cymbalyuk GS, Gaudry Q, Masino MA, and Calabrese RL. 2002. Bursting in leech heart interneurons: cell-autonomous and network-based mechanisms. J. Neurosci. 22(24): 10580–10592.